Deformation in the Three Gorges Reservoir after the first impoundment determined by GPS measurements*

DU Ruilin[1,2], QIAO Xuejun[1,2**], WANG Qi[1,2], XING Canfei[1,2] and YOU Xinzhao[1,3]

(1. Institute of Seismology, CEA, Wuhan 430071, China; 2. Laboratory of Crustal Movement and Earth Observation, Wuhan 430071, China; 3. Center for Analysis and Prediction, CEA, Beijing 100036, China)

Received August 3, 2004; revised September 20, 2004

Abstract A 6-year long GPS observation (1998—2003) indicates that crustal deformation in the Three Gorges area is less active at a marginally measurable rate of 0—5 mm/a relative to stable South China block. However, the impounding water in June 2003 has induced transient displacement at the Three Gorges dam and the emerging reservoir. GPS measurements after the first stage of water filling of the reservoir demonstrate that vertical subsidence close by Yangtze River is about 10—40 mm, and the horizontal displacement is less than 5—10 mm. The maximum subsidence induced by the impoundment is located in the segment of the reservoir from Maoping to Xiangxi. The water loading-induced deformation diminishes rapidly with the distance from banks of the reservoir. The overall pattern of transient deformation is consistent with the simulation result of Farrell, and is attributed to the elastic response of upper lithosphere crust to overlying water reservoir.

Keywords: Three Gorges, GPS, impoundment, deformation.

Currently, the ongoing Three Gorges Project (TGP) is the biggest hydraulic project in the world and the Three Gorges dam will be one of the highest dams. Standing 185 m high, it will be holding 3.92×10^{10} m^3 of water when completed in 2009. However, previous researches and historical records have shown that such a huge content of water might trigger minor and mediate earthquakes[1—4], because a decrease of friction on an active fault due to pore pressure diffuseness and enhanced water permeation could cause fault intermittent unlocking to release seismic energy[4,5—8]. To mitigate the potential hazard, a dense network for monitoring surface deformation has been jointly established by China Seismological Bureau and the investor of TGP[9] using GPS, precise leveling, gravity, EDM and strainmeter. Such effort to address to reservoir-induced deformation is unprecedented for the ongoing large reservoir in the world.

On June 1, 2003, the time of second phase of TGP, the water level of the reservoir reached 135 m above sea level with an additional water volume of 1×10^{10} m^3 within 15 days since the onset of filling water. It is urgent to understand if the impoundment completed in a short period would trigger earthquakes around this area.

After the water filling, the differential motion around the reservoir definitely means a change of the local stress field, which may be another mechanism responsible for reservoir-induced earthquakes[10]. It is possible to encourage the landslide of hill slope along the reservoir due to sudden stress disequilibrium especially between the reservoir basin and its shores.

The previous work on the water-loading deformation depended mainly on the theoretical modeling due to either the lack of suitable monitoring tools or unsufficient data[6—8,11—13]. Here we report an ongoing transient crustal movement based on our GPS data and show a displacement field of subsidence deformation at a large spatial scale, which will be useful to studies such as earthquake mechanism and controlled deformation by hydrological, atmospheric and oceanic processes.

1 GPS measurements and data process

As part of the monitoring system of the TGP-induced earthquake, the GPS network, established in 1998 around the TGP area, consists of two perma-

* Supported by National Natural Science Foundation of China (Grant Nos. 40274007 and 40304002), Seismological Union Fund of Chinese Seismological Bureau (103030, 602015), the Ministry of Science and Technology of China and the Special Fund of Three Gorges Project Exploiting Corporation

** To whom correspondence should be addressed. E-mail: whgps@public.wh.hb.com

nent stations at Badong and Xinshan, and 21 rover sites. Additional five fixed sites and 4 rover sites were set up in May 2003, a month before the water impoundment. A total of 32 GPS sites are spaced at an average interval of 15 km from Yichang to Badong and able to provide useful constrain on tectonic motion and active fault slip in TGP and its adjacent areas (Fig. 1).

All of the GPS pillars with markers for enforced centralization are built onto bedrock. GPS campaigns in total were carried out respectively in 1998, 1999, 2000, 2001, and intensified in June, July and Sept. of 2003.

Ashtech Z-12 and AOA Benchmark GPS receivers equipped with Choke-ring antenna were used throughout all surveys. A session of a consecutive 96-hour observation at each site was adopted for surveys from 1998 to 2001, and a session of 60-hour for the three surveys in 2003.

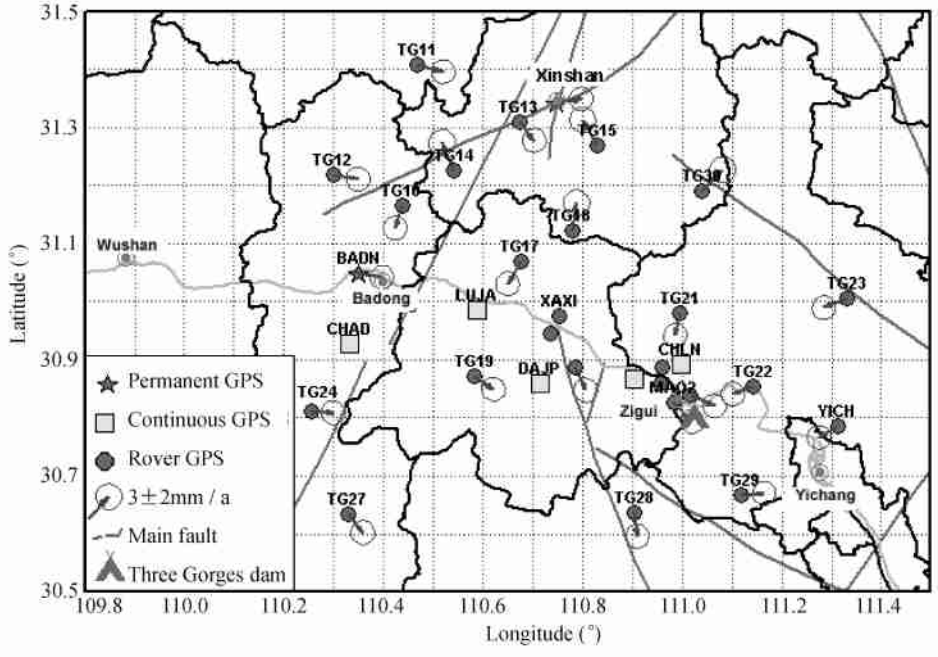

Fig. 1. GPS sites in the TGP area and horizontal velocity field relative to South China.

In order to yield daily solutions with GIPSY/OASISⅡ software, we analyzed simultaneously GPS data collected each day within a campaign in TGP, with continuous tracking data primarily contributed from 25 fiducial stations of Crustal Movement Observation Network of China (CMONOC) as well as 10 and more IGS stations in Asia[14, 15]. Through a combination of all daily solutions by the least squares algorithm, the estimated coordinates and velocities of GPS site are defined on the ITRF2000, a global reference frame. Uncertainties of relative positioning are less than 3—5 mm for the horizontal component and 9—12 mm for the vertical one, similar in precision as to the CMONOC[15]. Furthermore, uncertainties of site velocity are less than 2.0 mm/a and 3.2 mm/a respectively in horizontal and vertical components (Table 1), with a reasonable resolution to identify long-term tectonic or transient deformation in the Three Gorges area.

Meanwhile, we also used the Bernese V4.2 GPS software to process the same data set for a comparison. The Bernese-derived results that demonstrate the uncertainty of baseline determination respectively 1—3 mm and 3—6 mm in horizontal and vertical are similar to and perhaps slightly better than those yielded by GIPSY-OASIS Ⅱ in a sense of precision (we will present it else where). The inter-comparison between GIPSY and Bernses solutions suggests that the data analysis strategy is rational and solutions are robust.

Fig. 1 shows the GPS-derived horizontal velocity of the TGP area in a South China fixed reference frame. We realize it by least squares of all daily solutions, in which a square sum of velocity of WUHN, SHAO, GUAN, LUZH, XIAM, QION and YONG (the fiducial sites of CMONOC) as well as BADN and GUFU (two continuous GPS stations of TGP GPS network) is set to minimum. As a result, the Euler

vector of rotation of rigid South China block is given as follows: $\omega_x = -0.0501^\circ/\mathrm{Ma}$, $\omega_y = -0.2046^\circ/\mathrm{Ma}$ and $\omega_z = 0.2551^\circ/\mathrm{Ma}$[14,17]. The horizontal velocities of each site are about $0-3\pm2$ mm/a relative to South China block (Fig. 1). The relative displacements are very minor in terms of GPS data, consistent with the previous studies of geotectonic revealed by the geological evidence in South China[18,19]. Table 1 summaries the GPS velocities defined on the ITRF2000, South China fixed and NNR-NUVEL1A frames.

Table 1. Velocities of GPS sites in three different reference frames (Unit: mm/a)

GPS site	Longitude (°)	Latitute (°)	GPS observation (ITRF00)						NNR-NUVEL1A		GPS observation (in the Frame of South China)			
			E	RMS	N	RMS	U	RMS	E	N	E	RMS	N	RMS
GUFU	110.7	31.3	34.1	1.4	−12.4	1.4	2.0	2.2	23.4	−11.3	−0.20	1.61	0.91	1.64
BADN	110.3	31.0	35.0	1.4	−12.5	1.4	−1.1	2.2	23.4	−11.2	0.64	1.61	0.64	1.64
YICH	111.3	30.7	33.4	1.4	−11.7	1.4	2.0	2.4	23.3	−11.4	−0.83	1.70	1.73	1.67
TG11	110.4	31.4	34.7	1.5	−13.5	1.4	0.2	2.6	23.4	−11.2	0.39	1.73	−0.37	1.69
TG12	110.2	31.2	34.1	1.5	−12.7	1.5	1.0	2.6	23.4	−11.2	−0.26	1.78	0.43	1.72
TG13	110.6	31.3	33.3	1.5	−13.1	1.4	−0.1	2.5	23.4	−11.3	−0.93	1.72	0.18	1.69
TG14	110.5	31.2	32.9	1.4	−13.0	1.4	0.7	2.4	23.4	−11.2	−1.44	1.69	0.17	1.67
TG15	110.8	31.2	33.8	1.5	−13.8	1.4	0.4	2.5	23.4	−11.3	−0.47	1.73	−0.47	1.69
TG16	110.4	31.1	34.4	1.4	−14.5	1.4	−1.1	2.4	23.4	−11.2	0.06	1.70	−1.32	1.68
TG17	110.6	31.0	32.8	1.5	−13.3	1.4	−3.5	2.5	23.4	−11.3	−1.47	1.72	0.00	1.69
TG18	110.7	31.1	34.8	1.5	−14.3	1.4	−3.7	2.5	23.4	−11.3	0.59	1.73	−1.02	1.69
TG19	110.5	30.8	33.2	1.5	−11.6	1.4	0.5	2.5	23.4	−11.2	−1.03	1.72	1.57	1.69
TG20	110.7	30.8	34.0	1.5	−13.7	1.4	2.1	2.6	23.4	−11.3	−0.25	1.74	−0.42	1.69
TG21	110.9	30.9	30.5	1.5	−12.0	1.4	5.8	2.5	23.4	−11.3	−3.69	1.72	1.34	1.68
TG22	111.1	30.8	34.6	1.5	−12.1	1.4	0.6	2.5	23.4	−11.4	0.35	1.72	1.27	1.68
TG23	111.3	31.0	33.9	1.5	−13.5	1.4	0.3	2.6	23.3	−11.4	−0.24	1.74	−0.06	1.69
TG24	110.2	30.8	35.4	1.4	−12.1	1.4	0.8	2.5	23.5	−11.2	1.06	1.70	1.04	1.68
TG26	111.0	30.8	34.8	2.0	−13.4	1.9	−0.6	3.2	23.4	−11.3	0.61	2.36	−0.06	2.24
TG27	110.3	30.6	33.6	1.5	−12.4	1.4	−0.8	2.5	23.4	−11.2	−0.67	1.71	0.72	1.69
TG28	110.9	30.6	33.1	1.4	−14.0	1.4	−1.2	2.4	23.4	−11.3	−1.09	1.69	−0.64	1.67
TG29	111.1	30.6	34.8	1.5	−12.4	1.4	1.5	2.5	23.4	−11.3	0.60	1.72	0.95	1.68
TG30	111.0	31.1	35.1	1.5	−13.8	1.4	1.6	2.5	23.4	−11.3	0.89	1.73	−0.42	1.69

Note: the data of TG25 are invalid because the site did not work properly.

2 Modeling

We take two steps to model reservoir-induced deformation in terms of sudden displacement at all GPS sites. Firstly, on the basis of a high resolution InSAR-derived digital elevation model[20], the DEM digitized on a 1∶250000 topography map by the National Mapping Bureau, and the water level at various hydrological stations prior to the impoundment, the water volume that the TG reservoir holds at present is calculated. We select different areas and segments for simulation in order to improve estimation of incremental water volume after the impoundment. Taking into account the river course and topography along the river, we divide the reservoir into 21 segments from the dam upstream to Chongqing City. The total volume water held by the reservoir is estimated at 1.04×10^{12} m^3. Fig. 2 illustrates the systematic model of water volume associated with the impoundment. We ignored any increase in underground water in this model, considering that it may be very small and difficult to assess.

Secondly, the deformation in response to overlying water load is simulated, assuming that the underlying crust is elastic and isotropic. Therefore, the effect of water load on crust can be calculated through the integral with load and corresponding Green functions[21,22,13] like

$$u = \int_A G(|\boldsymbol{r} - \boldsymbol{r}'|)\rho(\boldsymbol{r}')H(\boldsymbol{r}')\mathrm{d}A, \quad (1)$$

where $\boldsymbol{r}$ is a coordinate vector of any point on surface, $\boldsymbol{r}'$ is the coordinate vector representing a point on the region A which is loaded by water. $\rho(\boldsymbol{r}')$ is the water density, $H(\boldsymbol{r}')$ the additional water level due to the impoundment at the point $\boldsymbol{r}'$, and G denotes the Green function. The vertical displacement can be expressed in terms of Green Function as follows:

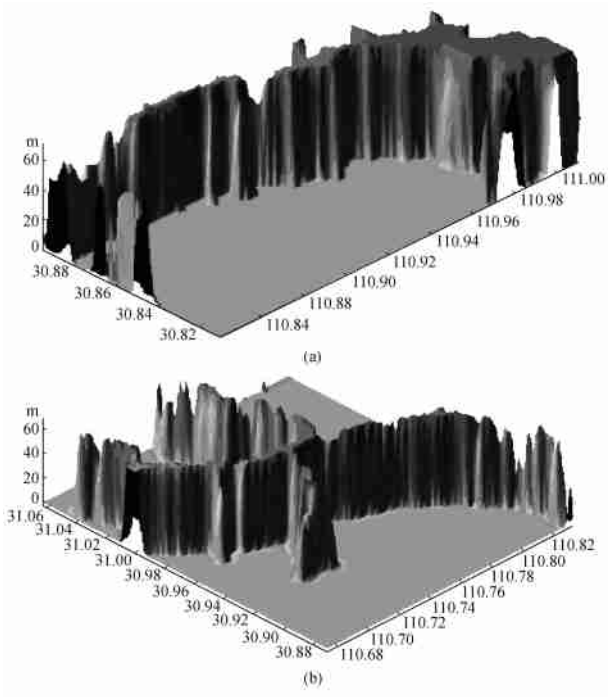

Fig. 2. The modeling water body increment after the first impoundment in TG reservoir. (a) In dam area, (b) in Xiangxi area.

$$GH(\theta) = \frac{\alpha}{M_e}\sum_{n=0}^{\infty} h_n P_n(\cos\theta), \qquad (2)$$

here, a denotes the radius of the earth, M_e is the mass of the earth. h_n represents the radial loading Love number, which represents the earth elastic property with a function of the spherical harmonic of degree n. $P_n(\cos\theta)$ stands for the n-th Legendre polynomial and θ is the angle between $\boldsymbol{r}$ and $\boldsymbol{r}'$.

In the simulation, we adopt the Gutenberg-Bullen model, one of the widely used standard earth models[21,23]. The loading Love number is calculated from Gutenberg-Bullen model[21]. In Eq. (2), the earth radius a is given as 6371000 m, the earth mass M_e is 5.9736×1024 kg, and a unit size of water loading is 46.7 m × 46.7 m × incremental height of water level (m), which should meet the need of simulation without loss of computation precision.

The subsidence in the regions of 106°24′E ~ 111°52′E (from dam to Chongqing) and 28°46′N ~ 31°56′N was simulated. Given that the crustal deformation caused by the surface loading with a total of mass (5.9736×1024 kg) is related to the angle θ and computer power is limited, we design a spherical grid of 2′ × 2′ outside the reservoir and 5″ × 5″ inside. Meanwhile, the loading deformation is also predicted for each GPS site. In general, our modeling shown in Fig.3 and Fig.4(c) is consistent with that given by Wang et al.[11,12].

3 Loading deformation

Fig. 4 (a) and (b) show the vertical changes of GPS sites in 3-D images one month and three months after water filling respectively, illustrating the spatial pattern of subsidence induced by water filling. The maximum of vertical displacement region is concentrated on the segment from the dam to Xiangxi where the surface subsidence close by the shore of reservoir is generally 20—40 mm, and the subsidence decreases to 10 mm at Badong (BADN), about 100 km upstream from the dam. The subsidence is inversely proportional to the distance off the river, and this is identical to the modeling results at 180 m water level

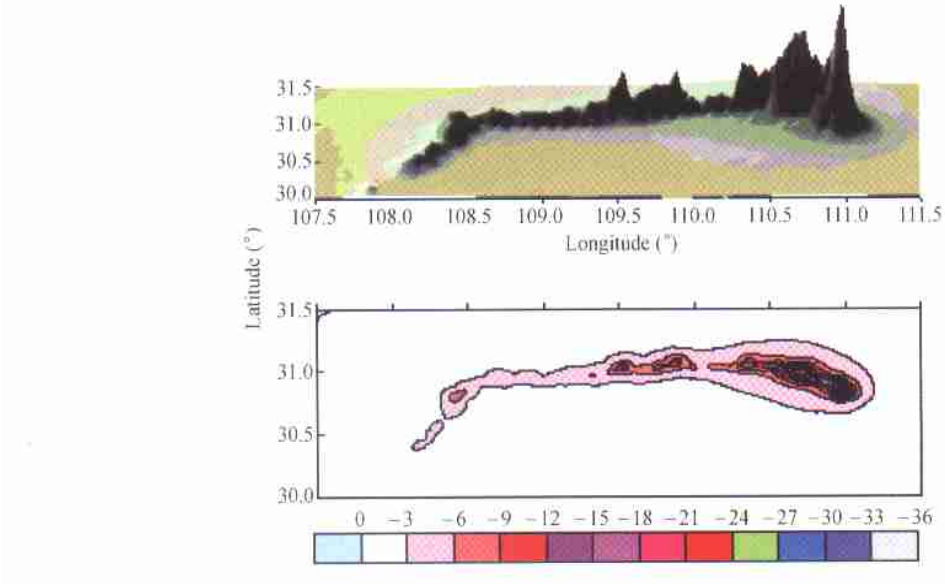

Fig. 3. The subsidence caused by water loading in the TG reservoir region (Unit: mm).

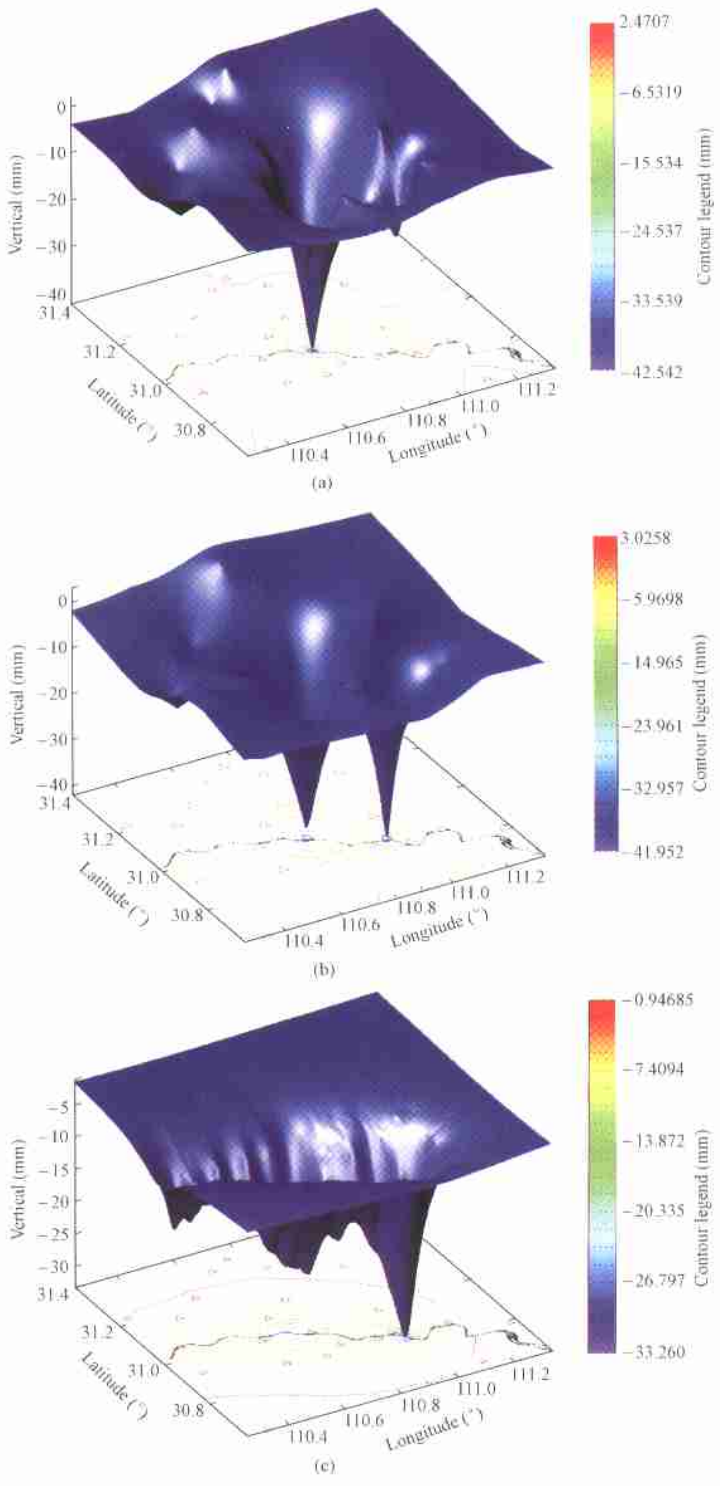

Fig. 4. The subsidence deformation of TGP reservoir region after the first impoundment (Unit: mm). (a) GPS observational result one month later; (b) GPS observational result three months later; (c) simulation result before and after the first impoundment.

of Gao[7] and Zeng[8] et al. The subsidence changes and its trend are difficult to distinguish when it is 3—5km away from the river central line, it might be that the increase of water is not enough and the affected area is comparatively small when the water line reached 135 m.

Comparison between our GPS-derived result and simulation models with Wang's researches[11, 12] measured at 138 m water level shows that the scope of peak value of modeling results and GPS are basically corresponding to each other. The dominating deformation areas are focused on Xiangxi stream and the third region of maximum subsidence is located at Badong segment.

The subsidence of 27.8 mm is predicted near by the dam (TPXN, YINX, etc.) here, the same as Wang's prediction of 28 mm. Repeated GPS measurements taken one month after the impoundment indicate that the vertical displacements in the south and north bank of the river are respectively about −31.1 mm and −27.1 mm, and −32.4 mm and −46.2 mm are given from re-measurements taken three months later. The maximal subsidence is predicted as 23.8 mm at Xiangxi (XAXI, GUOJ, etc.), whereas the GPS data imply that the subsidences at these sites are from 20.5 mm to 46.4 mm with uncertainties of about ±10 mm.

From the GPS data, the horizontal displacements associated to the impoundment are 0—5 mm with uncertainty of ±3 mm. No displacement is resolved with 95% confidence. So we conclude that the horizontal deformation by water loading must be minor if any, less than 5—10 mm.

In general, the GPS measurements tested against the numerical experiment show that both are consistent on magnitude of crustal deformation in the reservoir area, which implies that the transient subsidence is attributed to deformation response of elastic crust during a short period we were observing.

4 Discussions

For GPS, the uncertainty in vertical component originates from random errors and systematic biases which are usually associated with seasonal changes of environment. The vertical component is determined 2—3 times worse than the horizontal one. Principally, the GPS measurements around the impoundment were conducted in the same season (May and June of 2003), minimizing the seasonal effects on the vertical component by canceling and reducing some biases in common. But it should be noted that the observing environment in September 2003 is totally different from the one taken in May and June. The precision of the vertical component of loading deformation may be degraded slightly if the observation taken in autumn is combined with that in summer to infer the vertical displacement. Furthermore, the systematic deviations are reduced greatly once relative changes of vertical displacement in the region of interest are used to infer deformation. The fact that the measurements by GPS are basically identical to the prediction by the model implies that errors are, to some extent, under control without a damage on the final conclusion. Our GPS solution of the reservoir-induced deformation is robust enough for discerning any vertical displacement greater than 5 mm.

GPS sites are mainly distributed along the river bank; the crustal deformation related to the water loading maximizes primarily on the interior of the reservoir due to a deeper basin of reservoir, so the GPS observations can represent the subsidence deformation only in the targeted area instead of the whole area, especially the central area of the reservoir cannot be mapped directly by GPS. The subsidence displacement could be decreased with the increasing of the angle between surface sites and loading position. In order to get a more accurate map about the water loading subsidence, we might retrieve various observations such as GPS, leveling and gravity to improve the loading model. The combination of the GPS-derived results with the model is necessary to constrain parameters associated with the water loading.

The increased water capacity of 10.4×10^{10} m^3 by the available model is still an approximate estimation in general. The present calculation about total water loading is contaminated by some biases because of incomplete information in some regions. Another error source may originate from the neglect of enhanced subsurface aquifer especially at Xiangxi. Thus a better solution is expected if a more accurate DEM with resolution of 3 arc-seconds and bathymetric data of reservoir are available.

We assume that the crust is isotropic and the effect of water loading on the crust is uniform in a short period afterward. However, this assumption fails to represent all aspects of nature for each segment. Geophysical parameters of various models should be constrained tightly by "outputs" from direct measure-

ments so that our prediction on loading deformation is expected to be more accurate once the water level rises to 156 m in 2006 and 175 m in 2009.

The structure and strength of lithospheric crust determine its deformation behavior. Comparison of GPS solution with modeling gives away approximately the differences in tectonics and rock strength among various segments of the reservoir. The solid rock is on the segment closest to the TG reservoir dam, upstream to Jiuwangxi and Xiangxi based on studies of geological, morphology and petrous perviousness[6, 19, 24].

Pegmatite in Pre-Sinian outcrops widespread in the 16 km-width zone from the dam to Miaohe. Evidence of faulting and fissuring is rare there. Instead it is rigidly integrated, well-cementitious and poorly pervious. From Xiangxi to Guandu in Badong County, Paleozoic and Mesozoic carbonate with a layered structure is distributed mainly, accompanied by red clastic rocks of Zigui basin and coal bed. Faults in the vicinity of Xiangxi are well-developed and serious weathering is evident on the surface. Water permeation is readily under the circumstances of enhanced hydrostatic pressure. GPS sites at Xiangxi River are situated on a surface layer of clastic rock that is composed of marlite and gritstone and is much weaker than granite. That is the main reason for larger subsidence deformation at a rapid rate and a large scale as that derived by GPS.

5 Conclusions

The deformation field is determined precisely by the GPS measurements after the first filling of the Three Gorges Reservoir. We find that horizontal deformation related to the filling is small (0—5 mm), but vertical displacement is outstanding (10—40 mm). The dominated subsidence areas are localized on a belt of 3—5 km in width from the dam to Xiangxi. GPS solution about the deformation agrees with a prediction by the elastic deformation model. Although a slight difference exists between GPS and the modeling, we do not think that magnitude of vertical displacement determined by GPS differs obviously from its prediction, suggesting that the deformation observed in the short period of time is dominated by elastic response of upper crust to the surface loading.

Previous studies based on a layered half-elastic space model illustrated that the maximum subsidence was 70 mm and 90 mm respectively for the Danjiangkou and the Xinfengjiang reservoir in China, and 235 mm for the Koribar reservoir in Zambia[9]. A valley reservoir typical as the Three Gorges Reservoir has caused less magnitude and extent of local deformation than the lake reservoir. The transient deformation induced by the impoundment of the first phase of TGP is minor in magnitude and limited in narrow band. Thus, the probability of strong earthquake triggered by transient water loading in a short time (i.e. a couple of years) might be small. The local seismicity since the impoundment has also confirmed such a fact that actually, no earthquake greater than magnitude 3 has occurred there[26].

The crustal deformation response to water loading varies and associates with stress, pore pressure and water permeation. The deformation behavior and mechanism within the interior of lithosphere are different with depth. The overlying lower crust mostly responses elastically to the loading and deformation is recovered by unloading. Whereas underlying lower crust and upper mantle behave more visco-elastically, deformation will continue for a longer time after loading until a complete stress relaxes and is unrecovered if unloading. Therefore, it is possible to determine spatial and temporal characteristics to distinguish deformation mechanisms to shed a light on the dynamics of lithosphere of a stable craton such as South China by repeated GPS surveys, leveling and gravity data. As the representative example of controlled geophysical experiment, the TG impoundment process will provide a good chance to reveal regional dynamics and earthquake mechanism in addition to seismic hazard assessment.

References

1 Gupta H. K. Artificial water reservoirs and earthquakes: a worldwide status. Gerlands Beitrage Zur Geophysik, 1990, 99: 221—229.
2 Simpson D. W. Seismicity changes associated with reservoir loading, Engineering Geology, 1976, 10: 123—150.
3 Gough D. I., et al. Load-induced earthquakes at lake Kariba, Geophys. J. R. Astr. Soc., 1970, 21: 79—101.
4 Shen C. G. et al. Reservoir-induced earthquakes at Xinfeng River and its impacts on dam. Science in China (D), 1974, 2: 184—205.
5 Li A. R. et al. Collectivity environments and combination conditions of the earthquakes induced by Three Gorges Reservoir. In: Impacts of the Three Gorges Project on Ecosystem and Environments and Possible Countermeasures (in Chinese). Beijing: Science Press, 1987, 553—563.

6 Gao S. J. et al. The Lithosphere Stress Field and the Earthquake in the Three Gorges (in Chinese). Beijing: The Earthquake Press, 1992, 79—114.
7 Zeng X.C. et al. Analysis of the stress deformation field and pore pressure under water loads in the Three Gorges Reservoir. In: Impacts of the Three Gorges Project on Ecosystem and Environments and Possible Countermeasures (in Chinese). Beijing: Science Press, 1987, 585—595.
8 The Three Gorges Group Institute of Geodesy and Geophysics of Chinese Academy of Sciences. Gravity and strain fields in Three Gorges. In: Impacts of the Three Gorges Project on Ecosystem and Environments and Possible Countermeasures (in Chinese). Beijing: Science Press, 1987, 596—612.
9 Xing C. F. et al. Crustal deformation monitoring network for Three Gorges Project on Yangtze River. Journal of Geodesy and Geodynamics (in Chinese), 2003, 23: 114—118.
10 Yu T. L. Crustal deformation and reservoir-induced earthquakes. Crustal Deformation and Earthquake (in Chinese), 1991, 11: 8—16.
11 Wang H. Surface vertical displacements and level plane changes in the front reservoir area caused by filling the Three Gorges Reservoir. J. Geophys. Res., 2000, 105(13): 211—220.
12 Wang H. et al. Prediction of surface horizontal displacements and gravity and tilt changes caused by filling the Three Gorges Reservoir. J. Geod., 2002, 76: 105—114.
13 Boy J. P. et al. Time-varizable gravity signal during the water impoundment of china's Three Gorges Reservoir. Geophys. Res. Lett., 2002, 29(24): 53—1.
14 Wang Q. et al. Present-day crustal deformation in China constrained by global positioning system measurements. Science, 2001, 294: 574—577.
15 Wang Q. et al. Present-day crustal movement and deformation in China. Science in China (D) (in Chinese), 2001, 31(7): 529—536.
16 Niu Z. J. et al. Crustal movement observation network of China. Journal of Geodesy and Geodynamics (in Chinese), 2002, 22(3): 88—93.
17 Wang M. et al. Present-day crustal movement and activity block models in China. Science in China (D) (in Chinese), 2003, 33(suppl.): 21—32.
18 Zhang P. Z. et al. Present-day severe earthquakes and activity blocks in China. Science in China (D) (in Chinese), 2003, 33 (suppl.): 12—20.
19 Peng G.Z., et al. Impacts of the Three Gorges Project on reservoir banks' stability and their evaluating. In: Impacts of the Three Gorges Project on Ecosystem and Environments and Possible Countermeasures (in Chinese), Beijing: Science Press, 1987, 613—634.
20 Qiao X. J. et al. Acquisition of DEM Three Gorges area by INSAR. Journal of Geodesy and Geodynamics (in Chinese), 2003, 23(2): 122—127.
21 Farrell W. E. Deformation of the earth by surface loads. Rev. Geophys., 1972, 10: 761—797.
22 Mao W. Static response of the earth under surface mass loads. Acta Geophysiea Sinica (in Chinese), 1984, 27(1): 74—83.
23 Zhang S. Outline of Geophysics (in Chinese). Beijing: Earthquake Press, 1987, 182—183.
24 Yuan D. at el. The Study of Crust Stability in the Damsite and Surrounding Area of the Three Gorges Project (in Chinese). Wuhan: China University of Geosciences Press, 1996.
25 Li S. et al. First microquake swarm activity since storage in Three Gorges Reservoir (in Chinese). Journal of Geodesy and Geodynamics, 2003, 23(4): 75—79.